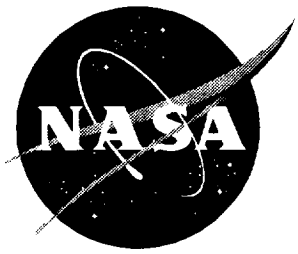

NASA Technical Memorandum 4767

A Feasibility Study To Control Airfoil Shape Using THUNDER

Jennifer L. Pinkerton and Robert W. Moses
Langley Research Center • Hampton, Virginia

National Aeronautics and Space Administration
Langley Research Center • Hampton, Virginia 23681-2199

November 1997

The use of trademarks or names of manufacturers in this report is for accurate reporting and does not constitute an official endorsement, either expressed or implied, of such products or manufacturers by the National Aeronautics and Space Administration.

Available electronically at the following URL address: http://techreports.larc.nasa.gov/ltrs/ltrs.html

Printed copies available from the following:

NASA Center for AeroSpace Information
800 Elkridge Landing Road
Linthicum Heights, MD 21090-2934
(301) 621-0390

National Technical Information Service (NTIS)
5285 Port Royal Road
Springfield, VA 22161-2171
(703) 487-4650

Summary

The objective of this study was to assess the capabilities of a new piezoelectric actuator to alter the upper surface geometry of a subscale airfoil to enhance performance. This new piezoelectric actuator called thin-layer composite-unimorph ferroelectric driver and sensor (THUNDER), recently developed at Langley Research Center, is manufactured to deform out of plane when under an applied voltage and, to date, has exhibited much larger displacements than other piezoelectric actuators. It was anticipated that attaching a THUNDER wafer to the upper surface of a small airfoil and actuating it to increase the camber of that surface when the airfoil was at positive angles of attack (above 2°) would extend the region of attached flow across the upper surface. Two common characteristics of all piezoelectric actuators, creep and hysteresis, however, pose challenges when THUNDER is used for airfoil shaping or other positioning applications.

For this study, a subscale airfoil model was designed, fabricated, and tested under two-dimensional flow conditions in a small tabletop wind tunnel. Sixty test conditions, consisting of combinations of five angles of attack, four direct current (dc) applied voltages, and three tunnel velocities, were studied. Results indicated that displacements of the upper surface of the airfoil were affected by the magnitude of the applied voltage, the tunnel velocity, the airfoil angle of attack, and the creep and hysteresis of the THUNDER wafer. Larger magnitudes of applied voltage produced larger wafer displacements. Wind-off wafer displacements were consistently larger than corresponding wind-on displacements; however, higher velocities produced larger displacements than lower velocities because of increased upper surface suction. Larger displacements were also recorded at higher angles of attack because of increased upper surface suction. Creep and hysteresis of the wafer were identified at each test condition and contributed to larger negative displacements for all negative applied-voltage conditions and larger positive displacements for the smaller, positive applied-voltage (+102 V) condition. An elastic membrane used to hold the wafer onto the upper surface hindered displacements at the larger magnitude positive applied voltage (+170 V). Both creep and hysteresis of the THUNDER wafer appeared bounded, based on the analysis of several displacement cycles. These results show that THUNDER can be used to alter the camber of a small airfoil under aerodynamic loads. Feedback control techniques may be useful in reducing the effects of creep and hysteresis.

Introduction

Changing the local flow field around an airfoil to enhance overall aircraft performance has always been a goal of aircraft designers. Historically, aircraft wings have been designed for a single flight condition and then modified to work for other flight conditions through the use of conventional control surfaces (such as ailerons and flaps), spoilers, and variable wing sweep. Variable wing sweep affects changes in the local flow field by altering the flow velocity perpendicular to the leading edge of the wing. The conventional control surfaces and spoilers affect changes in the flow field by directly varying the camber on certain regions of the wing, thereby causing changes in the baseline structural and aerodynamic characteristics of the entire wing. By developing a database that relates wing sweep or a commanded aileron/flap/spoiler deflection combination to a corresponding wing performance, overall aircraft performance parameters, such as lift-to-drag ratio and structural loading, may be tailored for the different flight conditions required.

During the past decade, many researchers have also started to look at adaptive material actuator systems for performance-enhancing shape control. Like the conventional control surfaces, these actuator systems (in this particular application) are designed to alter local wing shape (through camber and/or twist) to produce favorable structural and aerodynamic changes in the entire wing. However, unlike the conventional control surfaces, which have been used successfully for many years, shape-controlling adaptive material actuator systems are still in the development stage.

Adaptive Wing Concepts

Incorporation of leading- and trailing-edge control surfaces on aircraft was one of the first successful innovations in wing design following the first heavier-than-air flight in 1903. Common on aircraft since the 1920's, these camber-varying devices have been used primarily to improve low-speed performance during takeoffs and landings and to provide trim and maneuvering capability during flight. Attempts to utilize such devices for broader adaptive-camber-control purposes have also been made many times during this century. In 1916, the Sopwith Baby incorporated trailing-edge flaps that automatically deflected at lower speeds and decambered at higher speeds via a connection to restraining bungee cords. Between 1919 and 1926, Dayton Wright Aircraft and Army Air Services Engineering developed and flew aircraft that similarly incorporated mechanically activated adaptive wing concepts. In 1933 and 1934, the Westland Lysander was outfitted with independent inboard and outboard cross-connected slats that were interconnected with trailing-edge flaps. This concept provided low-speed maneuvering by means of an adaptive wing that automatically varied deflection with angle of attack. Also in the 1930's, sailplanes began to regularly incorporate manually controlled, camber-varying trailing-edge flaps

to optimize gliding and ascending performance. And during World War II, adaptive trailing-edge flaps were included on a number of fighters, such as the P-51 Mustang, to permit high-lift maneuvering in aerial combat situations (ref. 1).

Until the 1970's, however, use of the wing control surfaces for purposes other than maneuvering aircraft and achieving design-point camber control for landings, takeoffs, and trim was the exception rather than the rule. For military aircraft, material and control limitations had plagued further development, but breakthroughs in both technologies in the seventies eliminated these barriers. For commercial transports, fuel consumption concerns provided the impetus for change. In each case, aircraft designers in the early 1970's began to expand the airfoil-shaping application of the control surfaces to improve the off-design performance of the aircraft during the clean-wing (cruising) phases of flight (refs. 1–3). One such technique, flap scheduling, uses predetermined flap deflections at specific flight conditions to produce more desirable aerodynamic shapes (ref. 2). Aircraft that have benefited from variable-camber techniques like this one include the Advanced Fighter Technology Integration (AFTI)/F-111, the F-18, the X-29, and the Airbus A340 (refs. 1 and 2).

As indicated in the previous discussion, over the past 80 years, wing aerodynamic control surfaces have proven to be an effective and efficient system for maneuvering an aircraft and regulating loads. Providing such control is the primary function of these wing control surfaces. Therefore, any additional use of the control surfaces, such as active wing shaping for aircraft performance enhancement, is generally a secondary function. When control surfaces are asked to perform both of these functions simultaneously, two issues must be addressed: (1) not compromising the control-surface authority available to maneuver the aircraft and (2) not losing adequate control effectiveness (ref. 1). To date, an actively controlled aerodynamic control surface that performs both functions well enough to remove these issues from consideration has not been realized. Consequently, in situations where the control surfaces are faced with a multifunctional task, any secondary functions, such as airfoil shaping, must be limited so that the primary function is not compromised.

There are also two design-driving issues that must be addressed when dealing with multifunctional control surfaces: (1) producing a reliable, maintainable system and (2) obtaining performance improvements without an excessive increase in complexity and structural weight (ref. 1). Because of such concerns and the multifunctional limitations of the aerodynamic control surfaces, alternatives for active wing shape control are being studied. The use of adaptive material actuators as control effectors is one such alternative.

Adaptive material actuator systems are attractive for performance-enhancing shape control because they offer two advantages over the conventional control surfaces. First, shape control can be the primary function of these adaptive systems, and second, such shaping can be accomplished smoothly without the introduction of flow-disturbing hinge lines.

The first attempt at active aerodynamic shape control was conducted in the mid-1980's and involved the use of piezoelectric actuators to generate twist and camber on the surface of a plate (ref. 4). In the 1990's, as the piezoelectric materials technology grew and developed, the scope of the applications expanded from relatively small coupon-type models to scaled wind-tunnel models. Two examples of wind-tunnel applications are the Piezoelectric Aeroelastic Response Tailoring Investigation (PARTI) (refs. 5–8) and the Actively Controlled Response of Buffet Affected Tails (ACROBAT) (ref. 9) program, which sought to achieve wing flutter suppression and vertical tail buffeting alleviation, respectively, through the use of piezoelectric actuation. Other studies in the 1990's, primarily analytical, have focused on assessing the capability of the commercially available adaptive materials to create significant skin deflections (refs. 10–16).

To date, adaptive material actuators have been tested only in such research-related applications as those mentioned previously. Results so far indicate that, although the currently commercially available adaptive material actuators work well for both flutter suppression and buffeting alleviation (refs. 5–9, 17, and 18), they lack the strength to adequately control load-dominated phenomena, such as divergence (ref. 19), and the strength and out-of-plane displacement capability needed to create airfoil shape variations that can significantly alter aerodynamic characteristics (refs. 10–16).

A new adaptive material technology called thin-layer composite-unimorph ferroelectric driver and sensor (THUNDER) (ref. 20), developed at Langley Research Center within the past few years, has shown some promise for overcoming these barriers. In developing THUNDER, researchers at Langley combined a new materials technology and a new processing technique to produce an actuator with a greatly improved out-of-plane displacement capability. To date, much effort has been expended toward understanding the behavior of this new material under unloaded and statically loaded conditions. More complex loading conditions, however, have not been investigated, and research into the reliability and load capacity of THUNDER has only recently been initiated.

Goals of the Airfoil THUNDER Testing To Ascertain Characteristics (ATTACH) Project

The purpose of the current study was to begin the process of understanding the behavior of THUNDER under aerodynamic loading conditions and to ascertain the potential for using this new technology in airfoil shaping applications. To accomplish these goals, a two-phase test program was conceived. Phase I involved identification of two nonlinear characteristics (creep and hysteresis) and the reliability (in terms of performance repeatability and fatigue) of a single wafer of THUNDER. Phase II examined the ability of the wafer to alter drag by changing the geometry of an airfoil. This second phase was based on the premise that a single actuated THUNDER wafer attached to the upper surface of an airfoil could displace that surface enough to extend the region of attached flow.

Figures 1 and 2 illustrate the concept of airfoil shaping using THUNDER affixed to the upper surface of a symmetric airfoil near the leading edge and covered with a flexible membrane. Figure 1 shows the typical flow field with the airfoil set at a positive angle of attack (above 2°) and the THUNDER wafer unactuated. As identified in the figure, the flow remains attached to the upper surface of this nominal airfoil configuration only across a small region near the leading edge. The flow then separates because of the presence of a large adverse pressure gradient (ref. 21). Figure 2 shows the anticipated flow field over the same airfoil with the THUNDER wafer actuated up to meet the flow. With such an increase in camber of the upper surface, the onset of the large adverse pressure gradient would be delayed, allowing for a longer attachment region.

This paper presents the approach and preliminary findings of phases I and II, known collectively as the ATTACH project. A discussion of piezoelectric materials in general, including an overview of the types of piezoelectric actuators currently available, is presented first, followed by detailed descriptions of the test facility, test configurations, systems, and equipment used. Experimental results of the THUNDER technology evaluation tests are also presented.

Piezoelectric Adaptive Materials

Piezoelectric materials, which develop a strain when subjected to an electric field and vice versa, are currently among the most widely used adaptive materials. Unrestrained, these materials can expand or contract freely while under an applied voltage. However, when affixed to a host structure, the movement of a piezoelectric material is inhibited, resulting in structural deformation and a corresponding change in the loads for that host structure (ref. 22). Currently, piezoelectric materials are divided into two groups that differ by the direction in which they are able to affect a host structure. The first group, commonly called strain actuators, exhibits an in-plane displacement capability. The second group, a new generation of actuators, exhibits an out-of-plane displacement capability.

The conventional configuration for an in-plane displacement piezoelectric actuator consists of a single piezoelectric wafer sandwiched between two electrodes, as shown in figure 3. The relationship between an applied electric field and the corresponding behavior of a piezoelectric wafer is well documented (refs. 18, 22, and 23). However, this relationship is not always ideal because of the presence of nonlinear characteristics, such as depoling, hysteresis, and creep. Depoling refers to the reorientation of the dipoles within a piezoelectric material in a different direction from the original poling direction, with the degree of rotation of the dipoles affecting the response of the actuator. As the dipoles rotate from an original 90° orientation to a 0° orientation, the performance of the actuator is correspondingly reduced. Actuator response then increases as the dipoles continue toward a complete 180° rotation from the original position; however, in that 90° to 180° range, the actuator response to an applied voltage is opposite to that in the 0° to 90° range. Hysteresis is a typical characteristic of most electromechanical devices, and it results in a residual strain within the piezoelectric material. Creep is also a typical characteristic of electromechanical devices that appears as a slow deformation of the piezoelectric material when that material is subjected to a constant (zero-frequency) electric field for a prolonged period of time, particularly under high-strain conditions. For situations involving high frequencies, low applied voltages, and small deformations, the effect of these nonlinear characteristics is often assumed to be negligible. In most other cases, however, some form of correction would need to be applied to account for them (ref. 23).

Currently, several configurations exist for the standard in-plane displacement piezoelectric actuator. The basic configuration, called a piezoelectric patch, consists of one or more layers of piezoelectric wafers. These patches can be packaged in a protective coating for added durability. Increased actuation can be obtained by grouping multiple wafers into multiple layers, usually two or three deep. By stacking several of the actuators, an interim-type of actuator (called a piezoelectric stack) that possesses some out-of-plane displacement capability can be created.

Two actuators specifically designed to have an out-of-plane displacement capability are the unimorph and the bimorph, both of which incorporate the basic in-plane piezoelectric wafer previously discussed. As shown in

figure 4(a), a unimorph is made by bonding the wafer to a metal shim. When a voltage is applied across the wafer, the shim is forced to move with it, resulting in axial buckling and an out-of-plane displacement. Figure 4(b) illustrates the configuration for a bimorph, which is created by bonding together two oppositely poled piezoelectric wafers. In this case, an applied voltage across a shared electrode simultaneously expands one wafer and contracts the other, resulting in increased axial buckling and, therefore, an even larger out-of-plane displacement than can be obtained from the unimorph.

Recently, two actuators representing a new generation of out-of-plane displacement piezoelectric actuators have been developed: (1) reduced and internally biased oxide wafer (RAINBOW) (ref. 24) and (2) THUNDER. Both devices have configurations similar to the unimorph; however, they incorporate a prestressing phase during fabrication to set the final out-of-plane equilibrium position. Prestressing of the RAINBOW wafers is accomplished through a high-temperature chemical reduction of one surface. Prestressing of the THUNDER wafers begins by surface coating a raw piezoelectric wafer with a Langley-developed polyimide called LaRC™-SI. The coated wafer is then bonded on one side to a parabolically shaped "backup," which consists of alternating layers of a material, such as aluminum or steel, and the LaRC™-SI polyimide, as shown in figure 5. The new wafer is then vacuum bagged around a form to press the layers together and cured at an elevated temperature. Differences in the coefficients of thermal expansion for the polyimide, which hardens at a high temperature, and the other materials in the wafer result in final prestressing as the wafer cools (ref. 20). The strength and displacement capability of the THUNDER actuators are directly proportional and inversely proportional, respectively, to the number of material layers used in the backup. An illustration of the unrestrained movement of these out-of-plane actuators is shown in figure 6.

RAINBOW, the first of the new-generation actuators to be developed, possesses 10 times the displacement capability and 100 times the load capacity of the bimorphs. Comparisons between THUNDER and RAINBOW displacements and load capacities are not as easily defined, however. Displacement capability comparisons are difficult to make because THUNDER output varies with the type and number of backup layers used. Strength comparisons are even more difficult to make because, as previously mentioned, THUNDER load-capacity research is incomplete. A comparison between a 1.5-in-wide, 2.5-in-long, 0.012-in-thick, 9-layer-aluminum THUNDER wafer and a 1.25-in-diameter, 0.02-in-thick RAINBOW wafer is provided in figure 7. As indicated in the figure, this particular THUNDER wafer possesses up to 13 times the displacement capability of the RAINBOW wafer.

In general, the selection of an appropriate actuator group for use with different types of applications is based on four criteria: bandwidth, force, displacement capability, and ease of application. For applications seeking to control aeroelastic phenomena, bandwidth, force, and ease of application tend to be the major criteria; thus, in-plane actuators suffice. However, for airfoil shaping, displacement capability takes precedence. Therefore, out-of-plane displacement actuators, such as piezoelectric stacks, RAINBOW wafers, and THUNDER wafers, are most suited for this application. Selection of a specific actuator within the in-plane or out-of-plane displacement actuator group is then based on consideration of the individual characteristics of the actuators, including weight, life span (fatigue), and required maintenance.

As in the case of the conventional control surfaces, there are still many issues to address concerning the use of piezoelectric adaptive-material actuators for performance-enhancing shape control, including system complexity, reliability, and scaling effects. However, if such issues can be resolved, these actuators offer potential for use in future active systems, even on a full-scale aircraft.

Test Systems and Apparatus

Wind Tunnel

The wind tunnel used for the ATTACH project was the Flutter Research and Experiment Device (FRED), a tabletop wind tunnel operated by the Aeroelasticity Branch at Langley. This particular tunnel was selected for the study because it had already been proven effective for small-scale testing in 1993, when it was used to investigate the use of in-plane piezoelectric actuators for flutter suppression (ref. 18).

A photograph of the complete setup for the ATTACH project, with components of the FRED wind tunnel identified, is shown in figure 8. Figure 9 provides a side-view schematic of the wind tunnel. As shown in the figures, the FRED wind tunnel is an open-circuit tunnel with a 6- by 6-in. fully removable, Plexiglas[1] test section that also has a removable ceiling. Powered by a 2-hp motor, the wind tunnel is capable of operating at a maximum velocity of 125 ft/sec. A single honeycomb screen at the beginning of the contraction duct helps to smooth the flow before it reaches the test section.

[1]Registered trademark of Rohm & Haas Company.

ATTACH Testbed

The design of a testbed for the ATTACH project was driven by four specifications. First, it had to accommodate the 1.5-in-wide, 2.5-in-long, 0.012-in-thick, 9-layer-aluminum THUNDER wafer available for testing. Second, the span of the wafer had to appear infinite to the flow (e.g., two-dimensional flow) to simplify the analysis of the data. Third, the process for integrating the testbed into the test section needed to be simple to facilitate model changes and actuator performance checks. Finally, restraints on the movement of the actuated wafer needed to be minimized.

The final ATTACH testbed design is shown in figures 10 and 11. The ATTACH airfoil, shown in figure 10, consisted of a base airfoil, the THUNDER wafer, a thin fiberglass sheet, and a flexible latex membrane. The base airfoil was a 0.25-in-thick, 1.5-in-wide, 5-in-long Plexiglas symmetric airfoil that was positioned at approximately midheight in the tunnel test section, as depicted in figure 11(a). This airfoil was supported by two 0.25-in-thick, 10-in-long Plexiglas sidewall inserts that extended through 85 percent of the length of the test section, as shown in figure 11(b), creating a nearly two-dimensional flow condition between them. The THUNDER wafer was placed 0.125 in. aft of the base airfoil leading edge and extended from near 0 percent to approximately 50 percent chord. Only the wafer trailing edge was affixed to the base airfoil surface to permit relatively free expansion and contraction under an applied voltage. To further minimize wafer restraint, 0.06-in-deep notches were incorporated into the sidewall inserts in the areas that would be traversed by the lengthwise edges of the wafer. To smooth the airfoil-wafer interface, the fiberglass sheet was wrapped over the upper surface of the airfoil-wafer combination and held in place by the latex membrane, which covered both the upper and lower surfaces. A variable angle of attack mechanism was also included in the design. The entire assembly (sidewall inserts and ATTACH airfoil) could be slid easily in and out of the removed test section, and with the test section installed, minor adjustments could be made to the assembly by removing the test section ceiling.

For the two phases of testing mentioned earlier, two sets of the sidewall inserts were developed. These inserts differed only by the downstream mounting locations of the ATTACH airfoil model in the wind-tunnel test section. For phase I, the model was positioned near the ends of the sidewall inserts to permit maximum settling of the flow, as shown in figure 12. For phase II, the model was moved forward so velocity measurements could be taken sufficiently aft of the airfoil trailing edge to allow the wake to return to tunnel static pressure (ref. 25). This version of the testbed is shown in figure 13.

Displacement Measurement System

Measurement of both the precise positions of the THUNDER wafer in the tunnel at various angles of attack and the displacements caused by applied voltages required a very sensitive displacement measurement system. To eliminate disruptions in the flow around the airfoil, a nonintrusive, video-based measurement system called EPIX that can detect displacements as small as 0.0004 in. was ultimately selected to monitor the lengthwise-edge displacements of the wafer at 15 locations. These measurement locations along the wafer edge were evenly distributed in 0.167-in. increments. The measurement rates available from the EPIX system included a 30-Hz sample rate for durations of up to 1 min or a 10-Hz sample rate during continuous operation (ref. 26). Photographs of the setup for the system, which employed a single camera lens, a video junction box, and a computer rack, are shown in figures 8 and 14.

The EPIX system operates by first isolating the highest contrast image in the field of view of the camera and then producing a file that indicates the coordinates of the points defining that image with respect to predetermined reference positions (ref. 26). To provide the high contrast needed to isolate the camera-side edge of the wafer, that edge was painted with a coat of fluorescent paint and illuminated with ultraviolet light. A photograph of the model in the test section with the wafer edge illuminated is shown in figure 15.

Wake Velocity Measurement System

As mentioned previously, the purpose of phase II was to examine the drag-reducing potential of the THUNDER wafer. To obtain the data for this phase of testing, wake velocity measurements were taken by manually traversing a hot-film anemometer velocity probe in 0.125-in. increments through the center of the test section 3.70 in. aft of the airfoil trailing edge. This hot-film anemometer was part of a Kurz 443M air velocimeter, which also provided an analog display for visual readouts in meters per second.

Power Supply System

The following equipment supplied power to the THUNDER wafer: a function generator, an APEX Microtechnology Corporation PA85 power operational amplifier, and two International Power direct-current (dc) power supplies. The amplifier, preset with a gain of 17, allowed maximum input voltages of ±10 V; thus, the maximum output voltages from the amplifier, which were also the input voltages to the wafer, were limited to ±170 V. The corresponding maximum output current was 140 mA. Wiring connections to the wafer for the power supply system are shown in figure 16.

Wind-Tunnel Test Procedure

Identifying Material Characteristics

Phase I of the ATTACH project was performed to identify the creep, hysteresis, performance repeatability, and fatigue characteristics of the THUNDER wafer under aerodynamic loading. The two goals for this phase were to gain familiarity with the new THUNDER actuator technology before applying it as a tool in airfoil shaping and to identify variations in the response of the wafer to different aerodynamic loading conditions.

To begin this phase of the project, a baseline for the unconstrained performance of the wafer was determined by applying a 2-Hz, −200-V to +400-V sine wave load to the wafer, as depicted in figure 17. This magnitude was selected because it represented the usable voltage range established by the wafer poling boundaries. The resulting wafer displacements obtained over this input voltage range are shown in figure 18. As indicated in the figure, the wafer cycled through a maximum out-of-plane displacement range of 0.129 in. while following a distinct hysteresis curve. The remaining three material characteristics of interest, creep, performance repeatability, and fatigue, were not apparent because the response was dynamic and the load was applied for just a few cycles.

Upon completion of the baseline unconstrained performance tests, the THUNDER wafer was integrated into the phase I testbed and installed in the test section of the wind tunnel. Sixty conditions were then tested to identify the effects of both applied voltage and tunnel velocity on wafer behavior at various angles of attack. These conditions consisted of combinations of the following parameters: five angles of attack (−2°, 0°, +2°, +4°, and +6°), four steady-state dc input voltages (−102 V, +102 V, −170 V, and +170 V), and three tunnel velocities (wind off, 65.6 ft/sec, and 114.8 ft/sec). At each condition, the static input voltage signal pattern shown in figure 19(a) was applied, and displacement measurements were taken with the EPIX system. The 30-Hz sample rate was used for 2 sec after 0, 0.5, 1, 2.5, 5, 7.5, 10, 10.25, 10.75, 11.25, 12.75, 15.25, 17.75, and 20.25 min had elapsed to monitor any creeping of the material. The 15-sec increment after the first 10 min indicates the time required to change the sign of the applied voltage. The first 20 conditions (4 dc voltages at 5 angles of attack) were tested with wind off and established baseline displacement references for the remaining 40 wind-on conditions. A typical plot of the wafer response to the static input voltage signal is shown in figure 19(b). The displacement of the wafer caused by creep during the positive and negative applied-voltage periods was calculated by determining the difference between points C and B and F and E, respectively.

During this phase of testing, the reliability of the THUNDER wafer was also examined by monitoring performance repeatability and material fatigue. Comparisons of wafer displacements measured under identical angle of attack, applied voltage, and tunnel velocity conditions were used to estimate performance repeatability. The presence of any THUNDER material fatigue was identified after each day of testing by applying the maximum available input voltages (±170 V) to the wafer wind off and comparing the resulting displacements to the corresponding displacements obtained prior to any wind-tunnel testing.

Identifying Airfoil Shaping Effectiveness

With the objective of determining the ability of the THUNDER wafer to reduce drag over the airfoil, phase II tests were conducted at the same 40 wind-on conditions described for phase I. Through the use of the wake velocity profile technique described in reference 25, velocity measurements were taken by manually traversing a hot-film anemometer velocity probe in 0.125-in. increments vertically through the center of the test section sufficiently aft of the airfoil trailing edge to allow the wake to return to tunnel static pressure. Each profile took approximately 4 to 5 min to complete; however, creep and hysteresis measurements could not be correlated with the profiles because the ultraviolet lamps used for the measurement system were removed during this phase of testing to maximize space and eliminate the possibility of heat exposure.

Results and Discussion

Creep, Hysteresis, Performance Repeatability, and Fatigue Characteristics

The data obtained during phase I identified the presence of both creep and hysteresis of the wafer under wind-off (aerodynamically unloaded) and wind-on (aerodynamically loaded) conditions. Typical wafer displacements observed in response to five cycles of the ±102-V and ±170-V applied voltage patterns are shown in figures 22 and 21, respectively. The test conditions for both of these examples were wind off with the base airfoil model at 0° angle of attack. Creep is characterized by the increasing positive (up) and negative (down) displacements exhibited by the wafer while under constant positive and negative applied voltages, respectively. As previously discussed, these displacements are the B-to-C and E-to-F displacements illustrated in figure 19(b). Hysteresis is represented by the "looping" wafer displacement patterns. The shapes of the hysteretic curves in figures 22 and 21 differ from the one identified in figure 18 because of the vertical offsets introduced by the creep of the wafer. Dashed lines between the plots for the

five cycles identify these offsets. As expected, larger magnitude voltages produced correspondingly larger displacements, with positive voltages expanding the wafer away from the surface of the base airfoil and negative voltages contracting the wafer down toward the surface.

The primary difference between the results obtained for the conditions shown in figures 20 and 21 involved the variation in wafer response to the two different constant positive applied voltages. As shown in figure 20, for the lower voltage condition (+102 V), creep of the wafer occurred in the same direction as the initial displacement. This result was anticipated because the voltage was well within the poling boundaries. For the higher voltage condition (+170 V) shown in figure 21, however, the wafer exhibited a downward creep (negative displacement), a result opposite to what is normally expected. Typically, this type of behavior indicates that the wafer has depoled. However, because +170 V is also well within the poling boundaries of the wafer, this behavior was more likely caused by the presence of the latex membrane. For all positive applied-voltage conditions, when the wafer expanded upward, the membrane would stretch, imposing a force on the wafer proportional to the product of the displacement and "spring constant" of the membrane. For the +170-V case, the displacement of the THUNDER wafer apparently created a large enough membrane force to move the wafer back toward the surface of the base airfoil. Negative wafer displacements caused by both the −102-V and −170-V applied voltages were increased with the membrane present. Table 1 shows the relative effect of the membrane on the displacements achieved by the wafer. Residual strains introduced by hysteresis and creep also could have contributed to the changes exhibited in the displacements.

Table 1. Effect of Membrane on Wafer Displacements for Wind-Off Condition

Voltage, V	Displacements, in.		Difference, percent
	Membrane absent	Membrane present	
+102	+0.0242	+0.0199	17.8
+170	+0.0440	+0.0395	10.2
−102	−0.0105	−0.0208	98.1
−170	−0.0285	−0.0436	53.0

Wind-off versus wind-on (membrane present) wafer displacement comparisons at 0° angle of attack are shown in figures 22 through 25. Both creep and hysteresis were still apparent for the wind-on conditions, but the presence of the flow contributed to typically smaller positive displacements (both before and after creep) as compared to wind off for the same positive applied voltages. Displacements under negative applied voltages were larger for the wind-on conditions. Figures 26 and 27 compare the displacements obtained for only the two wind-on conditions at the ±102-V and ±170-V conditions, respectively, and reveal a second trend. Positive wafer displacements were larger at the higher tunnel velocity than at the lower velocity because of the increased suction on the upper surface of the ATTACH airfoil. Increased suction was also responsible for producing larger positive displacements at higher angles of attack, as shown in figure 28. This figure presents wafer displacements obtained at each of the five angles of attack for the +102-V, 65.6-ft/sec flow condition. In this case, some of the increased displacements also could have resulted from more of the wafer being shielded from the flow at the higher angles of attack. Figure 29 demonstrates the combined effect of increased velocity and a higher angle of attack at the +102-V condition. As expected, positive wafer displacements were larger at the higher velocity than at the lower velocity. However, because of the added influence of a +4° angle of attack, the positive displacements for both velocities were larger than those previously identified in figure 26 for the 0° angle of attack condition.

Comparisons of wafer displacements measured under identical conditions at different times during phase I identified discrepancies in the performance of the THUNDER wafer. One such comparison for the wind off, ±102-V, 0° angle of attack condition is shown in figure 30. These measurements were made 2 weeks apart, and as identified in the figure, they differed by as much as 0.01 in. To minimize the introduction of such discrepancies in the creep and hysteresis data presented earlier, only displacements measured on the same day were compared.

After testing for 2 weeks in the tunnel, the overall displacement performance of the THUNDER wafer began to noticeably degrade. During subsequent examination, no visible flaws were found, but a 33-percent (60-nF) drop in capacitance was discovered, and repoling returned the wafer to original performance. No further evidence of fatigue was encountered during the remaining month of testing. Thus, similar to other piezoelectric adaptive materials, the performance of THUNDER appears to be a function of capacitance. However, no material property life studies were performed to solidify this link.

Wake Velocity Effects

As a result of the effects of testing at low Reynolds numbers (173 883 and 304 295 for the 65.6-ft/sec and 114.8-ft/sec conditions, respectively), a possible interference from the sidewall inserts, the presence of flow

separation at higher angles of attack, and the omission of the wafer nonlinearities, reliable quantitative profile drag coefficients could not be obtained from the wake velocity data. Consequently, for purposes of this feasibility study, it was assumed that variations in drag were directly proportional to velocity changes in the wake of the model. Comparisons of wake velocity for different test conditions, therefore, provided qualitative indications of the drag-reducing potential of the THUNDER wafer for this subscale model.

The wafer trends identified in phase II were consistent with those from phase I. Positive applied voltages, which expanded the upper surface of the airfoil, had the effect of increasing the velocity (and, therefore, the momentum) in the wake, a result consistent with a decrease in drag. By increasing the tunnel velocity and/or the model angle of attack, even greater expansions of the upper surface and, therefore, larger wake velocities were obtained at the positive voltages. Negative applied voltages had the opposite effect on wake velocity (and, therefore, on drag). It should be noted that these wake velocity trends were obtained using only 44 percent of the maximum unloaded capability of the wafer because of the amplifier output voltage limitations. Thus, greater increases in the wake velocity (or decreases in drag) would be expected if that percentage was increased.

Concluding Remarks

Tabletop wind-tunnel tests were conducted to assess the feasibility of using a thin-layer composite-unimorph ferroelectric driver and sensor (THUNDER) wafer to alter the upper surface of a small airfoil. Surface position was measured with a nonintrusive video system at 15 stations along the chord. Upper surface position was clearly affected by aerodynamic loading, the voltage applied to the THUNDER wafer, and material creep and hysteresis. Aerodynamic loads on the wafer varied with angle of attack and affected the initial displacement of the wafer when the voltage was applied. However, the force output of the wafer appeared greater than the aerodynamic loads at all times. For most cases of constant applied positive voltages, the position of the upper surface would creep in the positive direction from the initial positive displacement. The elastic membrane used to hold the wafer onto the upper surface of the airfoil would hinder the positive displacement of the wafer when the maximum amplifier output voltage was applied. This undesirable impact may be avoided by selection of a nonelastic membrane that allows the wafer to expand fully. During constant applied negative voltages, the position of the upper surface would creep in the negative direction from the initial negative displacement. Comparisons of the displacement histories after each cycle of positive and negative applied voltages revealed the hysteresis of the wafer. After a few cycles, the hysteresis appeared to be bounded such that the wafer appeared to be settling into a more predictable displacement-voltage relationship. Based on the behavior of the wafer during this study, the effects of creep and hysteresis may be reduced through the use of feedback control techniques. Because positive displacements became larger during a constant positive applied voltage, it is anticipated that the voltage commanded by a controller would be smaller with time. Further study is required to verify the usefulness of feedback control in maintaining prescribed upper surface positions.

NASA Langley Research Center
Hampton, VA 23681-2199
May 21, 1997

References

1. Szodruch, J.; and Hilbig, R.: Variable Wing Camber for Transport Aircraft. *Prog. Aerosp. Sci.*, vol. 25, 1988, pp. 297–328.

2. Renken, Jürgen: Mission-Adaptive Wing Camber Control Systems for Transport Aircraft. AIAA-85-5006, Oct. 1985.

3. Redeker, G.; Wichmann, G.; and Oelker, H.-C.: Aerodynamic Investigations Toward an Adaptive Airfoil for a Transonic Transport Aircraft. *J. Aircr.*, vol. 23, no. 5, 1986, pp. 398–405.

4. Crawley, Edward F.; Warkentin, David J.; and Lazarus, Kenneth B.: *Feasibility Analysis of Piezoelectric Devices.* SSL 5-88, MIT, Jan. 1988.

5. Heeg, Jennifer; McGowan, Anna; Crawley, Edward; and Lin, Charrissa: The Piezoelectric Aeroelastic Response Tailoring Investigation: A Status Report. *Smart Structures and Materials 1995—Industrial and Commercial Applications of Smart Structures Technologies*, C. Robert Crowe, ed., SPIE, Vol. 2447, Mar. 1995, pp. 2–13.

6. Lin, Charrissa Y.; Crawley, Edward F.; and Heeg, Jennifer: Open Loop and Preliminary Closed Loop Results of a Strain Actuated Active Aeroelastic Wing. AIAA-95-1386, Apr. 1995.

7. Heeg, Jennifer; McGowan, Anna; Crawley, Edward F.; and Lin, Charrissa: The Piezoelectric Aeroelastic Response Tailoring Investigation. *International Forum on Aeroelasticity and Structural Dynamics 1995—Proceedings*, Royal Aeronaut. Soc. (London), 1995, pp. 8.1–8.11.

8. McGowan, Anna-Maria R.; Heeg, Jennifer; and Lake, Renee C.: Results of Wind-Tunnel Testing From the Piezoelectric Aeroelastic Response Tailoring Investigation. AIAA-96-1511, Apr. 1996.

9. Moses, Robert W.: Active Vertical Tail Buffeting Alleviation on a Twin-Tail Fighter Configuration in a Wind Tunnel. *International Forum on Aeroelasticity and Structural Dynamics*, CEAS, June 1997, pp. 269–276.

10. Ehlers, S. M.; and Weisshaar, T. A.: Static Aeroelastic Behavior of an Adaptive Laminated Piezoelectric Composite Wing. *A Collection of Technical Papers—AIAA/ASME/ASCE/AHS/ASC 31st Structures, Structural Dynamics, and Materials Conference*, Part 3, Apr. 1990, pp. 1611–1623.

11. Ehlers, S. M.; and Weisshaar, T. A.: Static Aeroelastic Control of an Adaptive Lifting Surface. *J. Aircr.*, vol. 30, no. 4, July–Aug. 1993, pp. 534–540.

12. Weisshaar, Terrence: Active Aeroelastic Tailoring With Advanced Materials. *31st Aircraft Symposium*, Japan Soc. Aeronaut. & Space Sci., Nov. 1993, pp. 34–45.

13. Muller, Mark B.: Transonic Drag Reduction Through the Use of Induced Strain Actuators to Form an Adaptive Airfoil. M.S. Thesis, Perdue Univ., May 1994.

14. Muller, Mark B.; and Weisshaar, Terrence A.: Maximizing Deflections Produced by Induced Strain Beam-Like Actuators for Transonic Drag Reduction. *AIAA/ASME Adaptive Structures Forum—Technical Papers*, 1994, pp. 388–401.

15. Leeks, Tamara J.; and Weisshaar, Terrence A.: Optimizing Induced Strain Actuators for Maximum Panel Deflection. *Proceedings of the AIAA/ASME Adaptive Structures Forum*, 1994, pp. 378–385.

16. Leeks, Tamara J.; and Weisshaar, Terrence A.: Optimization of Unsymmetric Actuators for Maximum Panel Deflection Control. *Smart Structures and Materials 1995—Smart Structures and Integrated Systems*. Inderjit Chopra, ed., SPIE, Vol. 2443, Feb.–Mar. 1995, pp. 62–74.

17. Lazarus, Kenneth B.; Crawley, Edward F.; and Lin, Charrissa Y.: Fundamental Mechanisms of Aeroelastic Control With Control Surface and Strain Actuation. *Proceedings of the 32nd AIAA/ASME/ASCE/AHS/ASC Structures, Structural Dynamics, and Materials Conference*. AIAA, 1991, pp. 1817–1831.

18. Heeg, Jennifer: *Analytical and Experimental Investigation of Flutter Suppression by Piezoelectric Actuation*. NASA TP-3241, 1993.

19. Layton, Jeffrey B.: An Analysis of Flutter Suppression Using Adaptive Materials Including Power Consumption. AIAA-95-1191-CP, 1995, pp. 299–305.

20. Hellbaum, Richard F.; Bryant, Robert G.; Fox, Robert L.; Jalink, Antony, Jr.; Rohrbach, Wayne W.; and Simpson, Joycelyn O.: Thin Layer Composite Unimorph Ferroelectric Driver and Sensor. U.S. Pat. 5,632,840, May 27, 1997.

21. Anderson, John D., Jr.: *Introduction to Flight*. Third ed., McGraw-Hill Book Co., 1989.

22. Weisshaar, Terrence: Aeroservoelastic Control Concepts With Active Materials. *ASME International Mechanical Engineering Congress Exposition, Special Symposium on Aeroelasticity and Fluid/Structure Interaction Problems*, Nov. 1994.

23. Crawley, Edward F.; and Anderson, Eric H.: Detailed Models of Piezoceramic Actuation of Beams. *J. Intell. Mater. Sys. & Struct.*, vol. 1, Jan. 1990, pp. 4–25.

24. Haertling, Gene H.: Rainbow Ceramics—A New Type of Ultra-High-Displacement Actuator, *American Ceram. Soc. Bull.*, vol. 73, no. 1, Jan. 1994, pp. 93–96.

25. Rae, William H., Jr.; and Pope, Alan: *Low-Speed Wind Tunnel Testing*. John Wiley & Sons, 1984.

26. Burner, A. W.: Model Deformation Measurements at NASA Langley Research Center. *RTO Symposium on Advanced Aerodynamic Measurement Technology*, AGARD-CP-601, 1997, pp. 34-1–34-9.

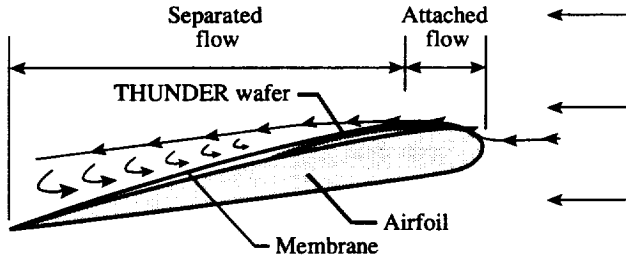

Figure 1. Streamline representation for nominal airfoil (wafer unactuated).

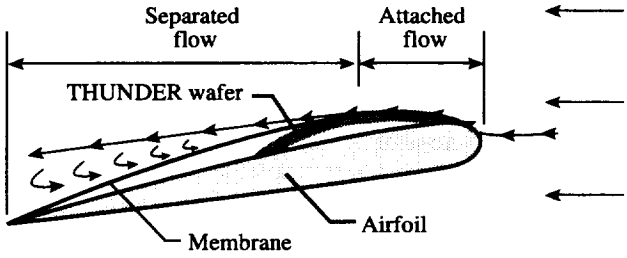

Figure 2. Anticipated streamline representation with altered upper surface geometry (wafer actuated).

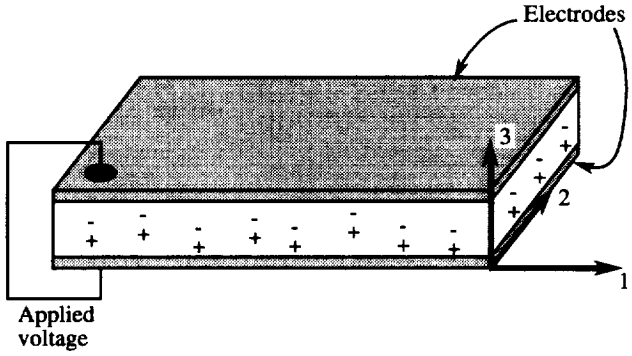

Figure 3. Conventional configuration for in-plane displacement piezoelectric actuator.

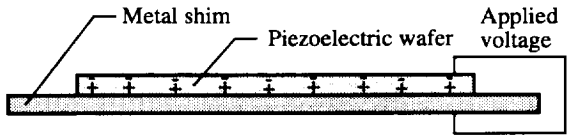

(a) Unimorph.

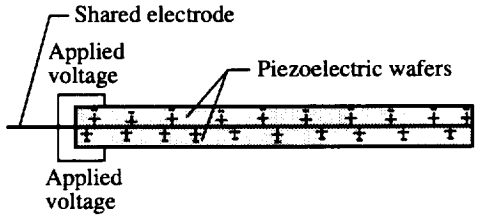

(b) Bimorph.

Figure 4. Configurations for unimorph and bimorph piezoelectric actuators.

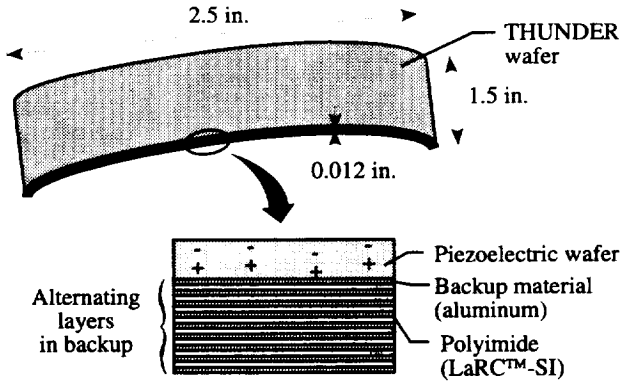

Figure 5. Isometric view of THUNDER wafer with enlargement of side layering (not to scale).

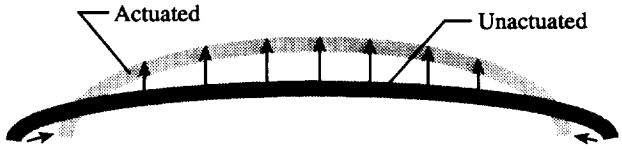

Figure 6. Unrestrained positive actuation of typical THUNDER wafer.

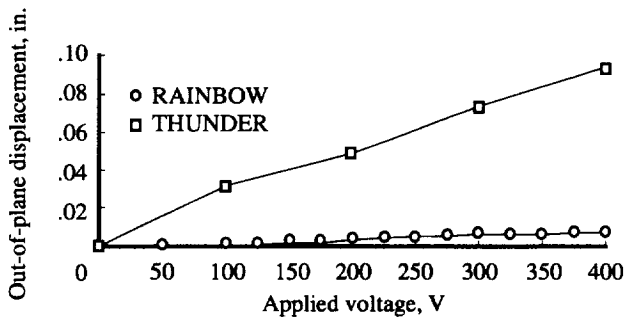

Figure 7. Comparison of out-of-plane displacements achieved by 1.5-in-wide, 2.5-in-long, 0.012-in-thick, 9-layer-aluminum THUNDER wafer and 1.25-in-diameter, 0.02-in-thick RAINBOW wafer.

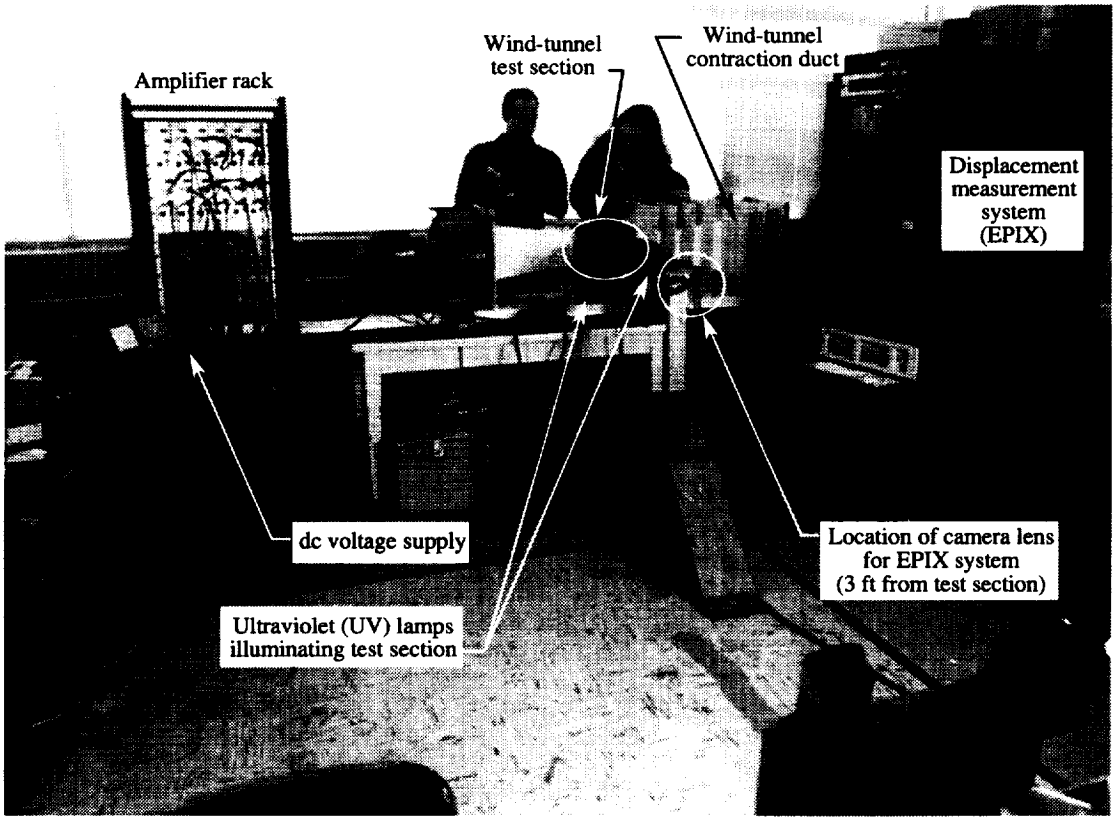

Figure 8. Photograph of ATTACH project experimental setup.

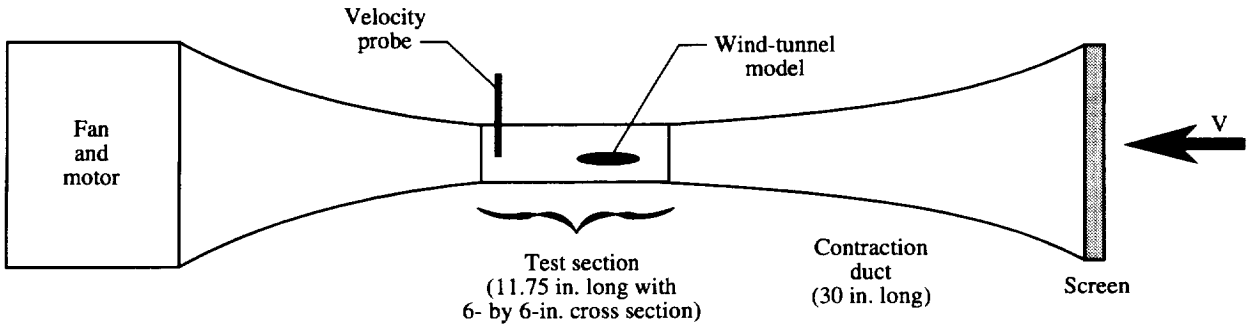

- Airfoil supported by two vertical end-plate inserts
- Tunnel limits: velocity = 125 ft/sec

Figure 9. Side view of Flutter Research and Experiment Device (FRED) wind tunnel.

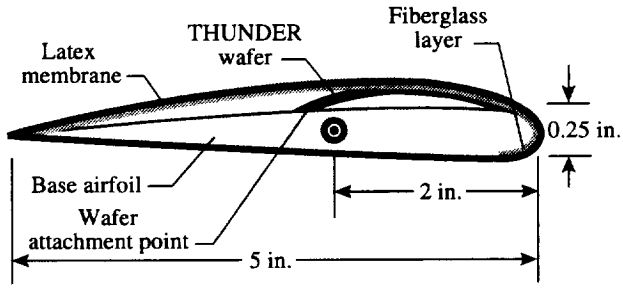

Figure 10. Cross section of ATTACH airfoil model.

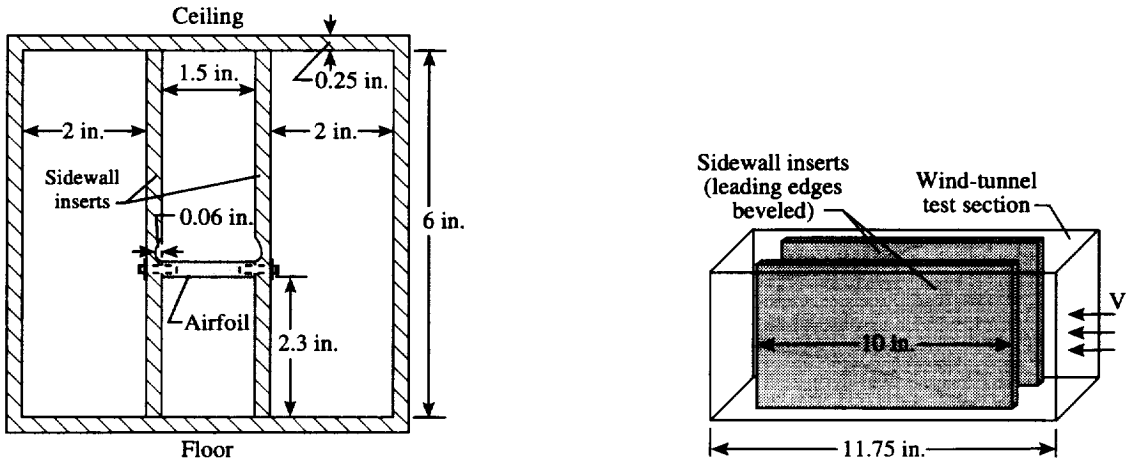

(a) Looking downstream. (b) Isometric view.

Figure 11. Wind-tunnel test section.

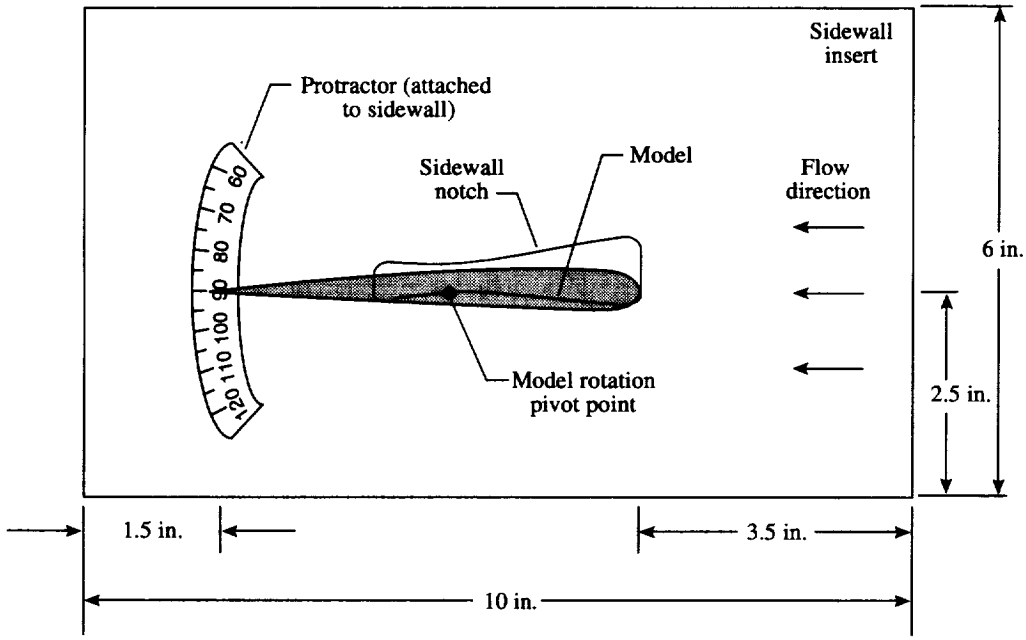

Figure 12. ATTACH testbed configuration for phase I.

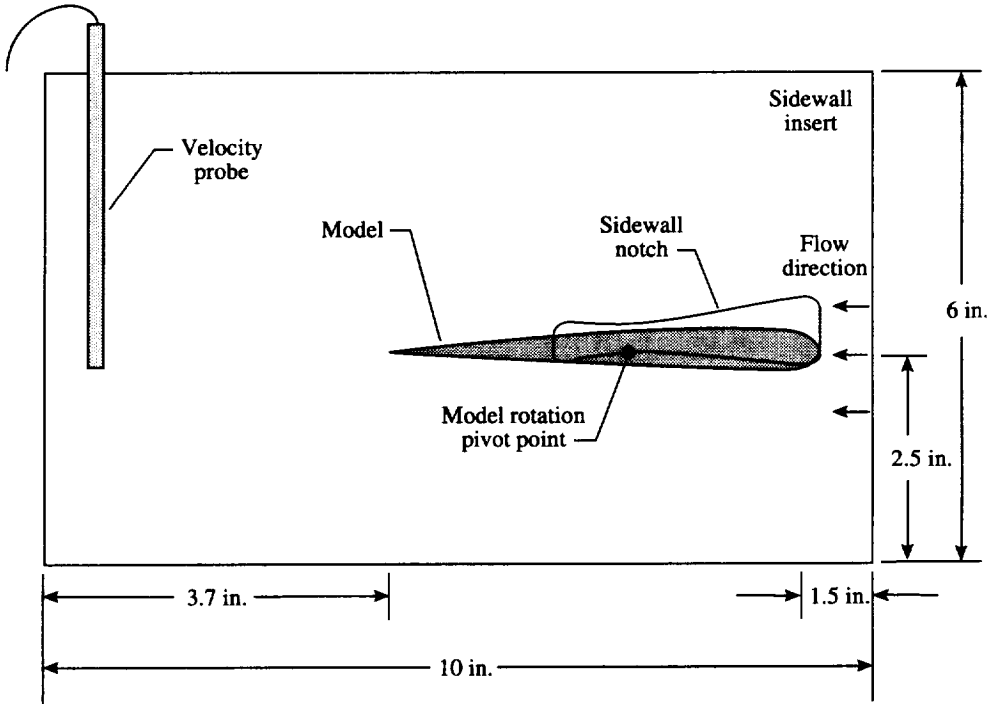

Figure 13. ATTACH testbed configuration for phase II.

Figure 14. EPIX system computer rack.

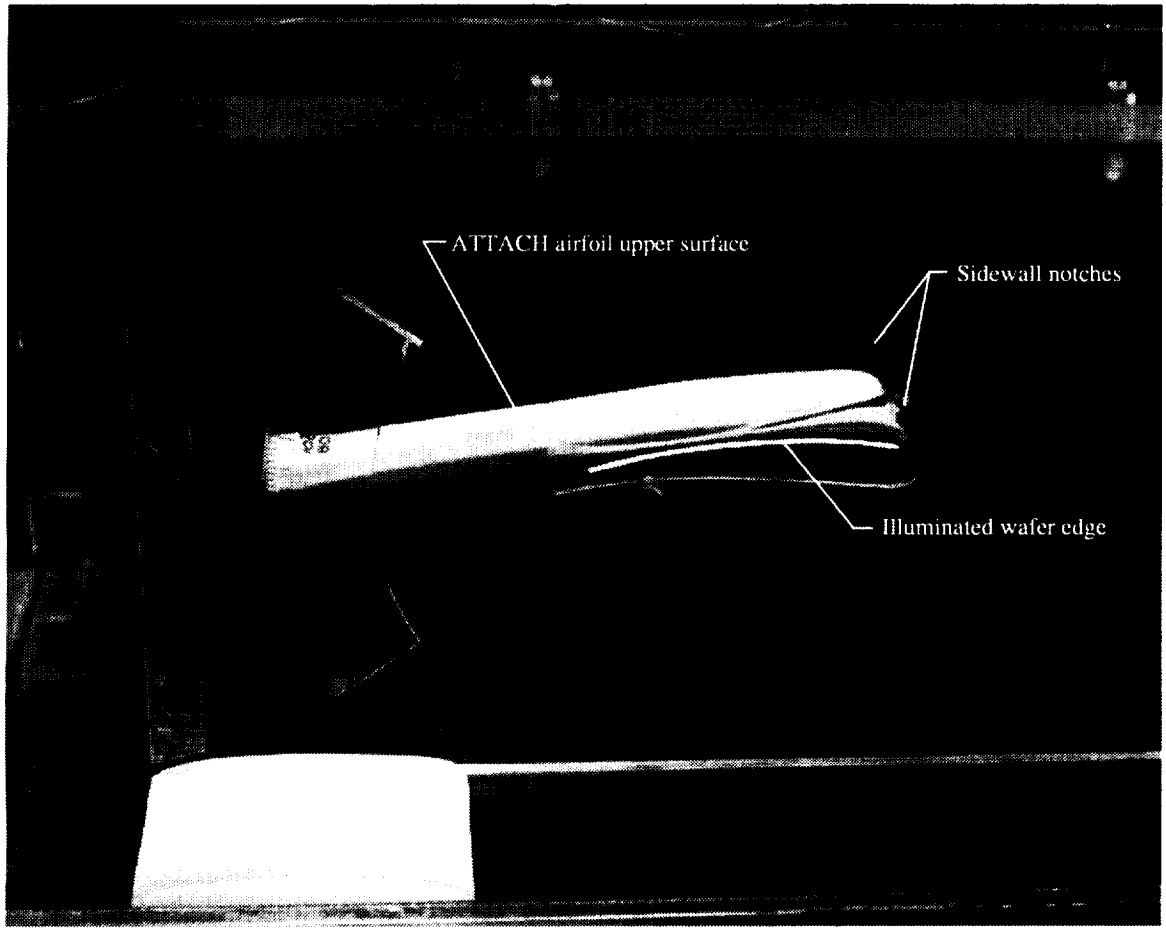

Figure 15. Photograph of ATTACH model in FRED.

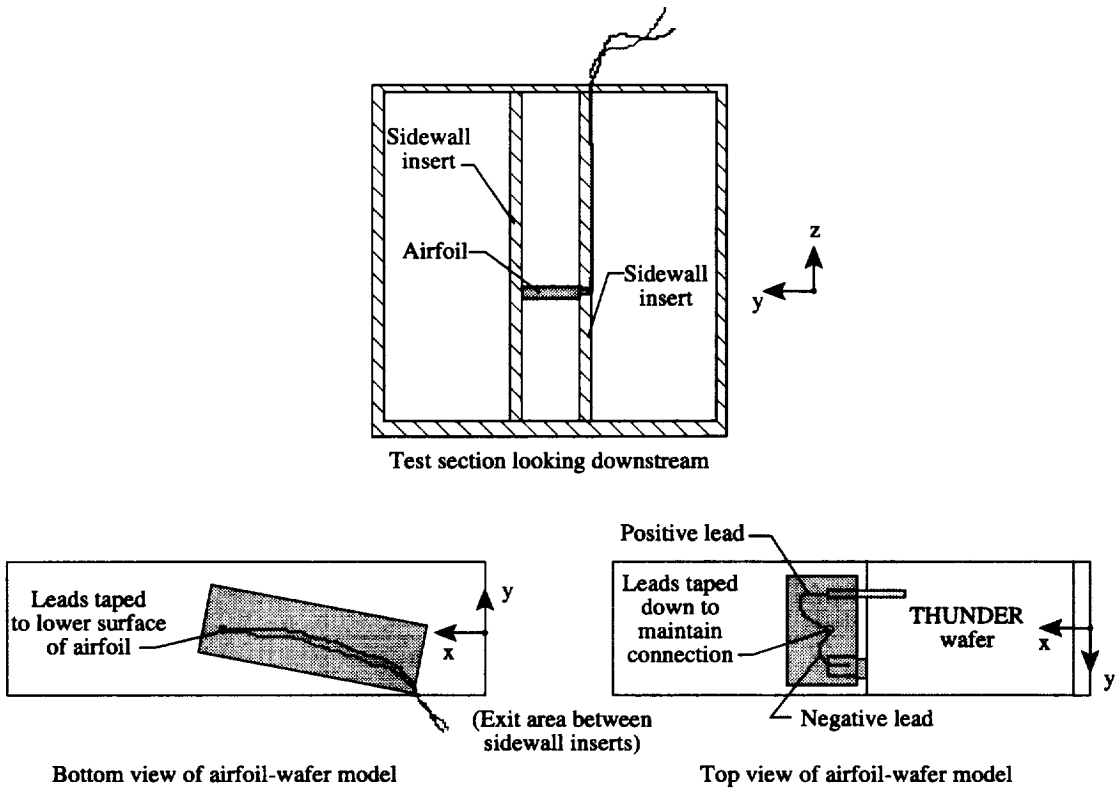

Figure 16. Schematic of THUNDER wafer wiring connections.

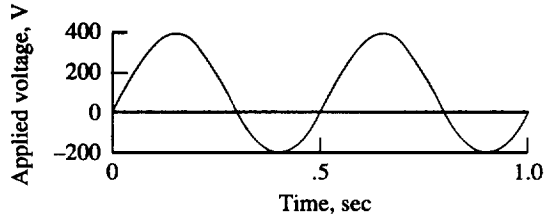

Figure 17. Input voltage signal used for performance-evaluation testing.

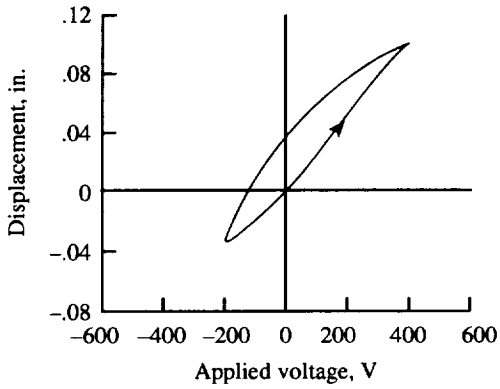

Figure 18. THUNDER wafer displacements and hysteresis that resulted from dynamic actuation.

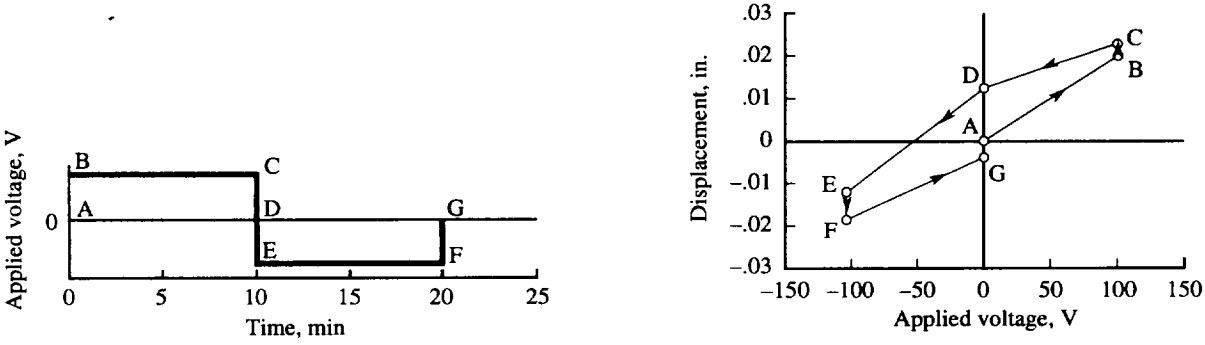

(a) Input voltage.

(b) Typical wafer response.

Figure 19. Input voltage signal used for phase I testing. Creep = B to C and E to F.

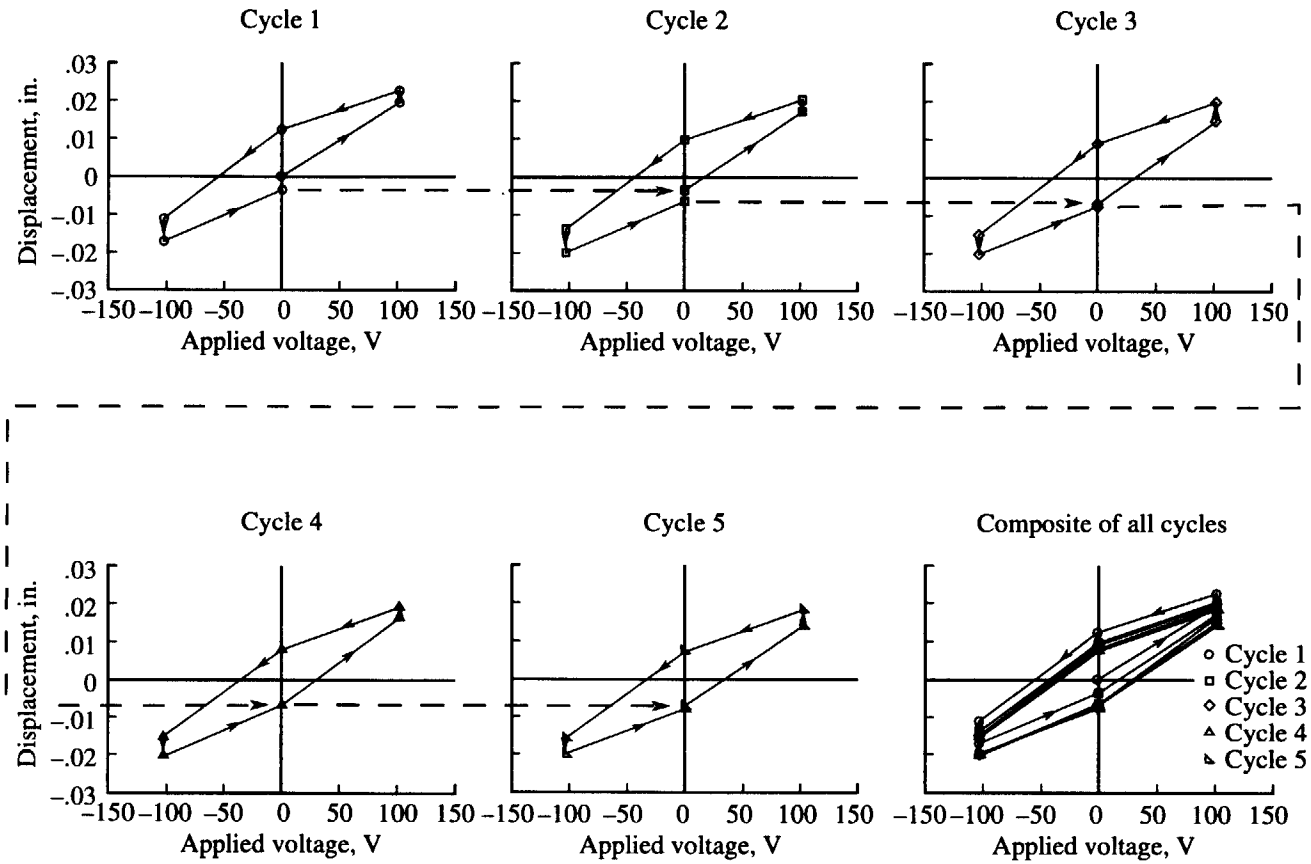

Figure 20. Typical wafer displacement pattern in response to five cycles of applied voltage, wind off, ±102 V, $\alpha = 0°$.

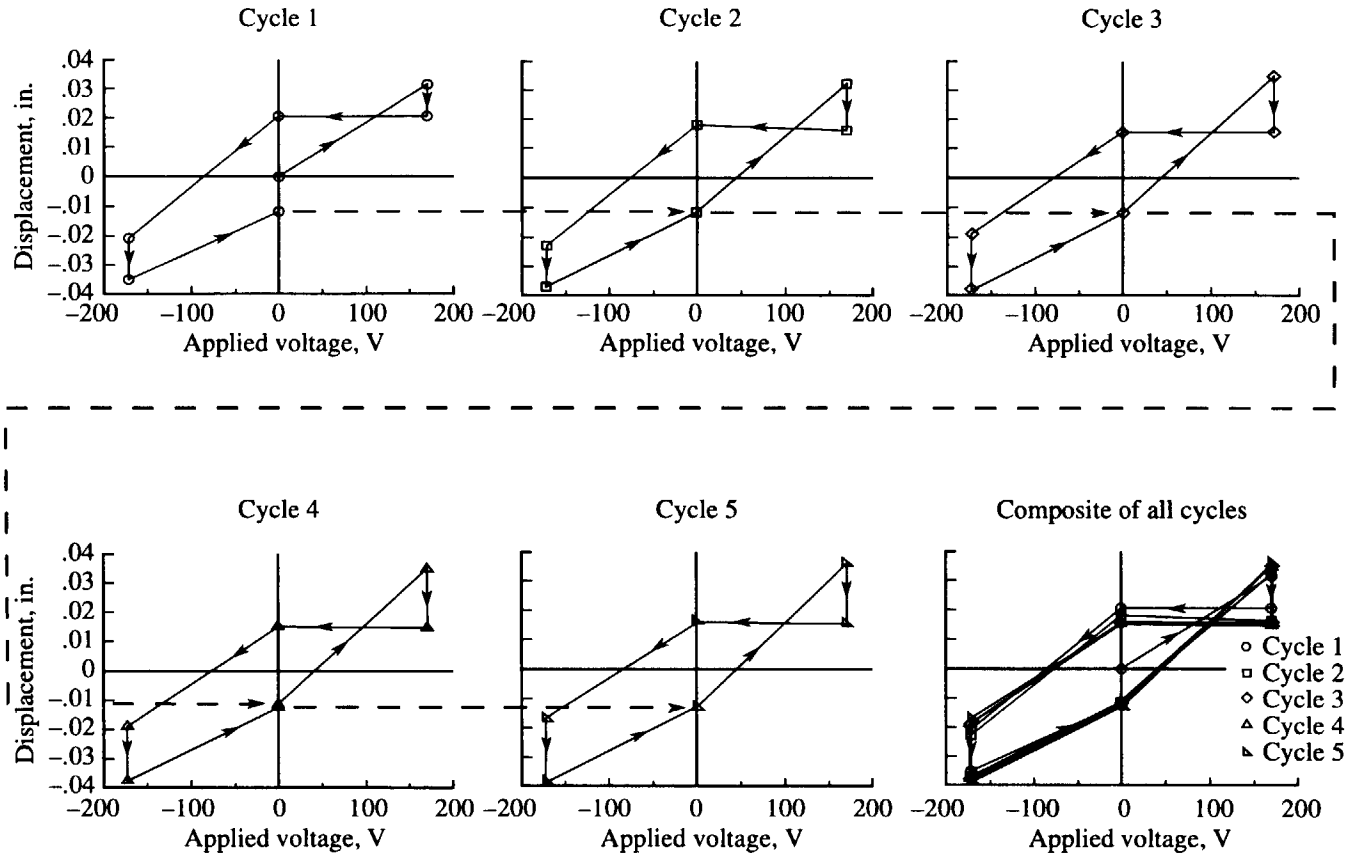

Figure 21. Typical wafer displacement pattern in response to five cycles of applied voltage, wind off, ±170 V, $\alpha = 0°$.

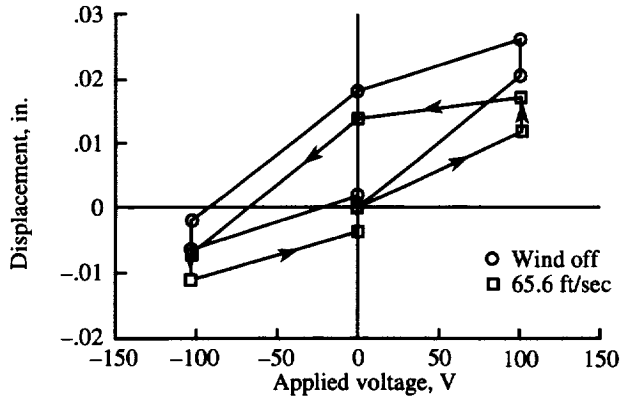

Figure 22. Wafer displacement changes caused by 65.6 ft/sec aerodynamic loading, ±102 V, $\alpha = 0°$.

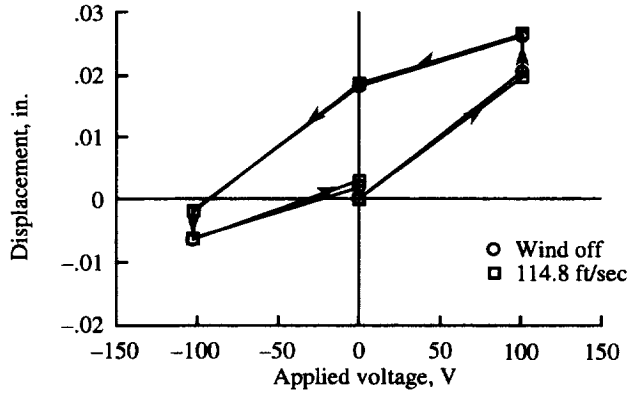

Figure 23. Wafer displacement changes caused by 114.8 ft/sec aerodynamic loading, ±102 V, $\alpha = 0°$.

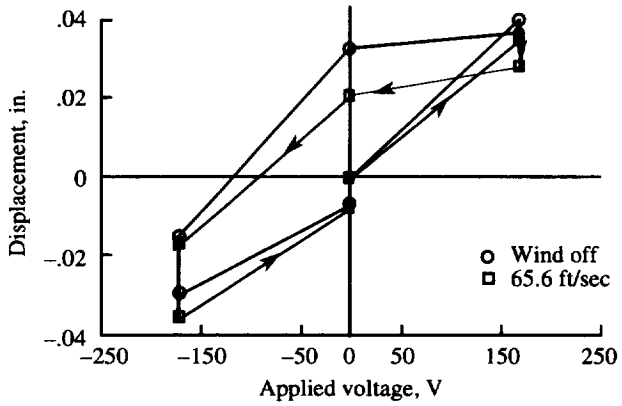

Figure 24. Wafer displacement changes caused by 65.6 ft/sec aerodynamic loading, ±170 V, $\alpha = 0°$.

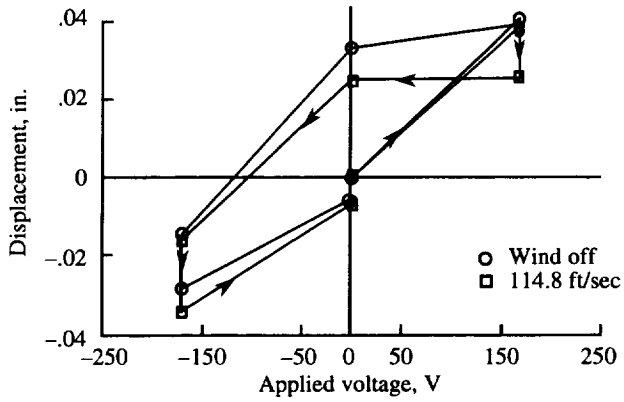

Figure 25. Wafer displacement changes caused by 114.8 ft/sec aerodynamic loading, ±170 V, $\alpha = 0°$.

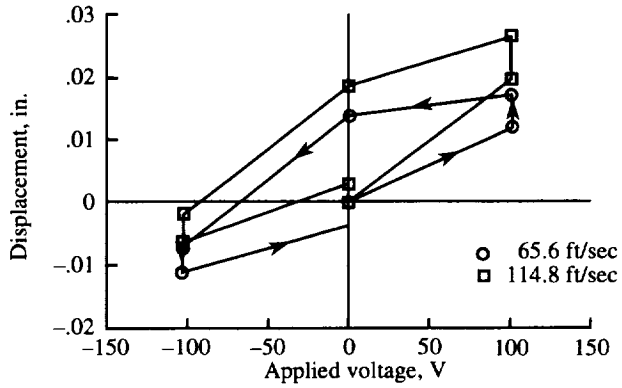

Figure 26. Wafer displacements obtained at 65.6 ft/sec and 114.8 ft/sec, ±102 V, $\alpha = 0°$.

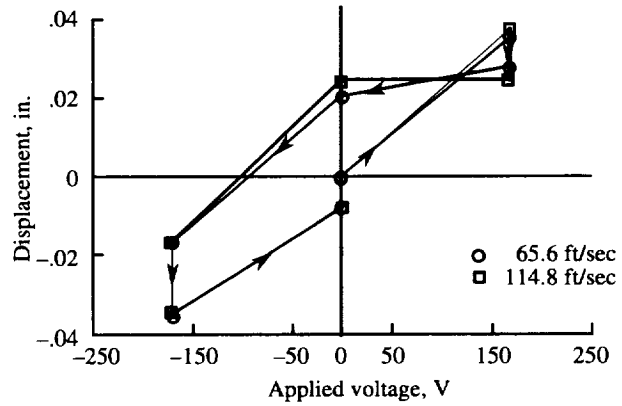

Figure 27. Wafer displacements obtained at 65.6 ft/sec and 114.8 ft/sec, ±170 V, $\alpha = 0°$.

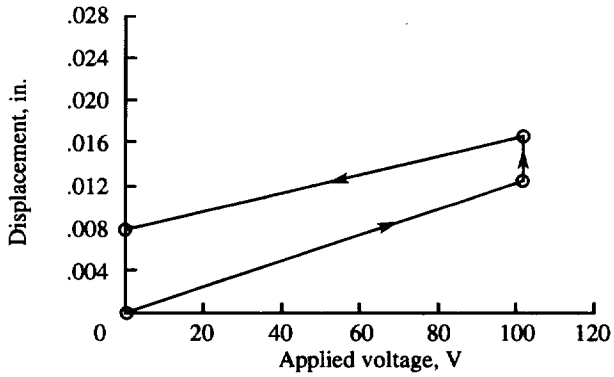

(a) $\alpha = -2°$.

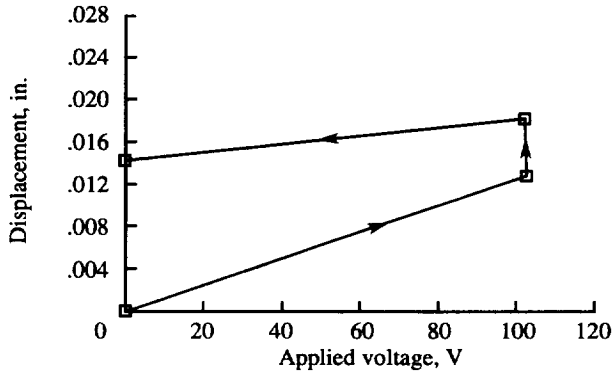

(b) $\alpha = 0°$.

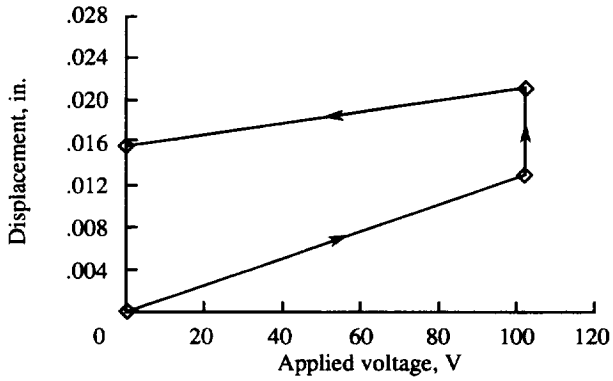

(c) $\alpha = +2°$.

Figure 28. Effect of angle of attack on wafer displacements, +102 V, 65.6 ft/sec.

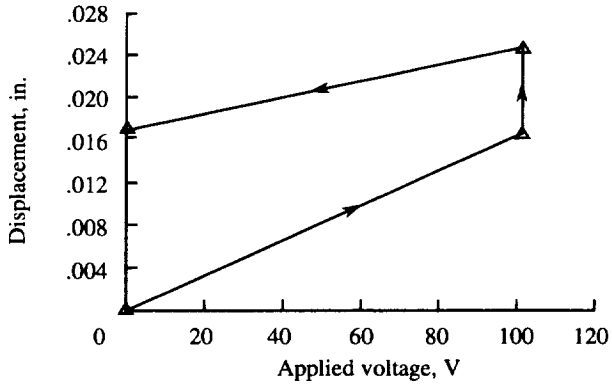

(d) $\alpha = +4°$.

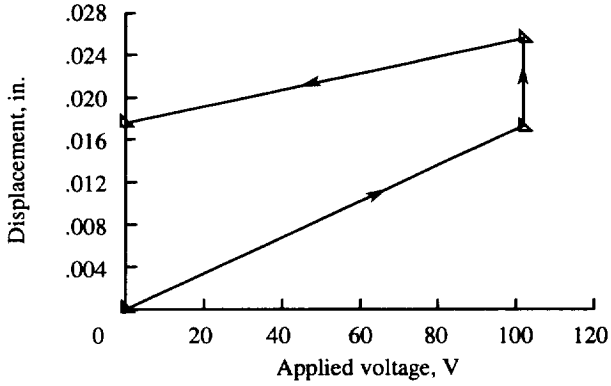

(e) $\alpha = +6°$.

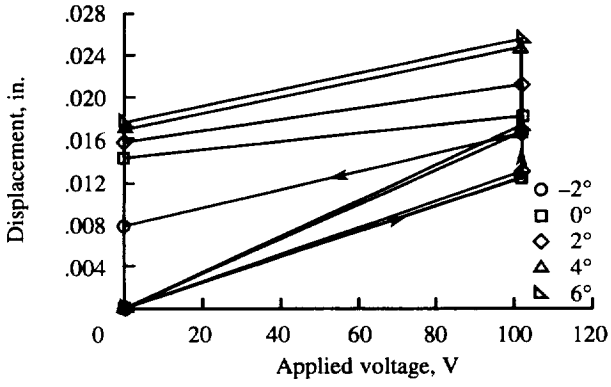

(f) Composite of all angles of attack.

Figure 28. Concluded.

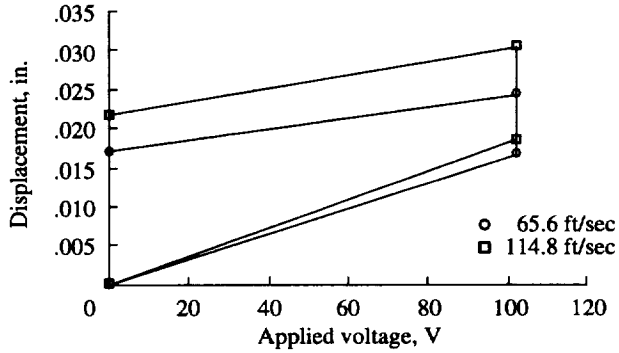

Figure 29. Wafer displacements obtained at 65.6 ft/sec and 114.8 ft/sec, +102 V, $\alpha = +4°$.

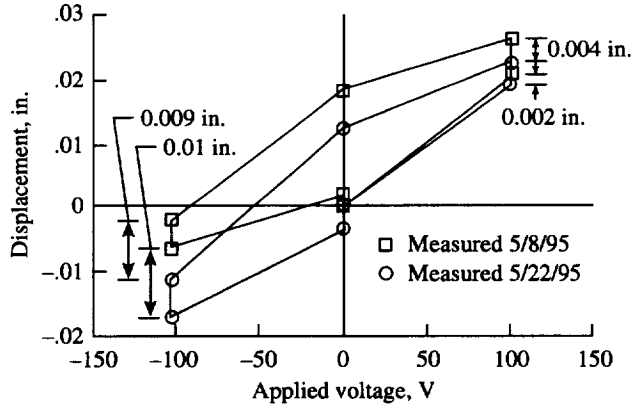

Figure 30. Wafer displacements obtained for wind off, ±102 V, $\alpha = 0°$.

REPORT DOCUMENTATION PAGE

Form Approved
OMB No. 0704-0188

1. AGENCY USE ONLY *(Leave blank)*	2. REPORT DATE	3. REPORT TYPE AND DATES COVERED
	November 1997	Technical Memorandum

4. TITLE AND SUBTITLE
A Feasibility Study To Control Airfoil Shape Using THUNDER

5. FUNDING NUMBERS
WU 505-63-50-13

6. AUTHOR(S)
Jennifer L. Pinkerton and Robert W. Moses

7. PERFORMING ORGANIZATION NAME(S) AND ADDRESS(ES)
NASA Langley Research Center
Hampton, VA 23681-2199

8. PERFORMING ORGANIZATION REPORT NUMBER
L-17544

9. SPONSORING/MONITORING AGENCY NAME(S) AND ADDRESS(ES)
National Aeronautics and Space Administration
Washington, DC 20546-0001

10. SPONSORING/MONITORING AGENCY REPORT NUMBER
NASA TM-4767

11. SUPPLEMENTARY NOTES

12a. DISTRIBUTION/AVAILABILITY STATEMENT
Unclassified–Unlimited
Subject Category 05
Availability: NASA CASI (301) 621-0390

12b. DISTRIBUTION CODE

13. ABSTRACT *(Maximum 200 words)*

The objective of this study was to assess the capabilities of a new out-of-plane displacement piezoelectric actuator called thin-layer composite-unimorph ferroelectric driver and sensor (THUNDER) to alter the upper surface geometry of a subscale airfoil to enhance performance under aerodynamic loading. Sixty test conditions, consisting of combinations of five angles of attack, four dc applied voltages, and three tunnel velocities, were studied in a tabletop wind tunnel. Results indicated that larger magnitudes of applied voltage produced larger wafer displacements. Wind-off displacements were also consistently larger than wind-on. Higher velocities produced larger displacements than lower velocities because of increased upper surface suction. Increased suction also resulted in larger displacements at higher angles of attack. Creep and hysteresis of the wafer, which were identified at each test condition, contributed to larger negative displacements for all negative applied voltages and larger positive displacements for the smaller positive applied voltage (+102 V). An elastic membrane used to hold the wafer to the upper surface hindered displacements at the larger positive applied voltage (+170 V). Both creep and hysteresis appeared bounded based on the analysis of several displacement cycles. These results show that THUNDER can be used to alter the camber of a small airfoil under aerodynamic loads.

14. SUBJECT TERMS	15. NUMBER OF PAGES
Piezoelectric actuators, THUNDER, Airfoil shaping, Creep, Hysteresis	30
	16. PRICE CODE: A03

17. SECURITY CLASSIFICATION OF REPORT	18. SECURITY CLASSIFICATION OF THIS PAGE	19. SECURITY CLASSIFICATION OF ABSTRACT	20. LIMITATION OF ABSTRACT
Unclassified	Unclassified	Unclassified	